



Simulating the impacts of ship emissions on coastal air quality: Importance of a high-resolution emission inventory relative to cruise- and land-based observations

Jingbo Mao ^a, Yan Zhang ^{a,b,c,*}, Fangqun Yu ^d, Jianmin Chen ^{a,b}, Jianfeng Sun ^a, Shanshan Wang ^{a,b}, Zhong Zou ^e, Jun Zhou ^f, Qi Yu ^a, Weichun Ma ^a, Limin Chen ^{a,**}

^a Shanghai Key Laboratory of Atmospheric Particle Pollution and Prevention (LAP3), Department of Environmental Science and Engineering, Fudan University, Shanghai 200438, China

^b Shanghai Institute of Eco-Chongming (SIEC), Shanghai 200062, China

^c Institute of Atmospheric Science, Fudan University, Shanghai 200438, China

^d Atmospheric Sciences Research Center, State University of New York, 251 Fuller Road, Albany, NY 12203, USA

^e Pudong New Area Environmental Monitoring Station, Shanghai 200135, China

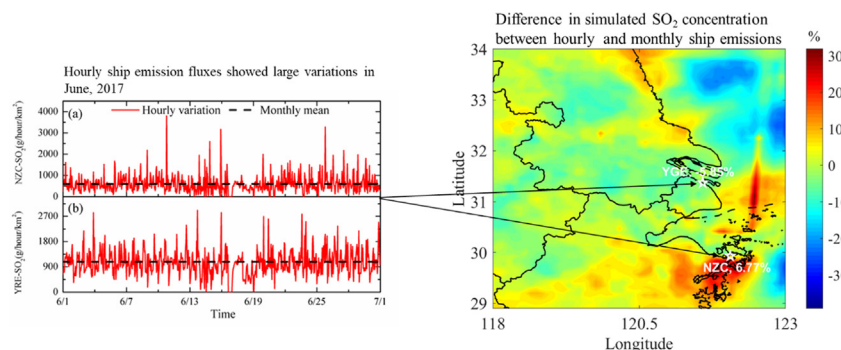
^f Ningbo Environmental Monitoring Center, Ningbo 315012, China



HIGHLIGHTS

- Hourly ship emissions showed large variations, especially near ports.
- Simulations were evaluated by on-line cruise- and coastal land-based measurements.
- Realtime emissions are crucial to explore realistic impacts of shipping traffic.

GRAPHICAL ABSTRACT



ARTICLE INFO

Article history:

Received 25 December 2019

Received in revised form 2 April 2020

Accepted 3 April 2020

Available online 20 April 2020

Editor: Pingqiang Fu

Keywords:

Ship emissions

Coastal air quality

High-resolution emission inventory

ABSTRACT

This work studied the impacts of ship emissions at a high temporal resolution on the real-time concentrations of PM_{2.5}, NO₂, and SO₂ in urban harbors and coastal sea areas, taking the Yangtze River Delta (YRD) as an example. The WRF-Chem model with 3 nested grids and ship emissions derived from an automatic identification system (AIS) were combined to simulate the air quality. The AIS data showed significant temporal fluctuations in ship emissions, with hourly mean fluxes of approximately 1082.41 ± 444.41 and 593.55 ± 404.95 g/h/km² near ports and in the channel waters of the YRD, respectively. The monthly mean contributions of shipping emissions reached 80.72% (2.15 ppbv) and 81.79% (8.79 ppbv) to ambient SO₂ and NO₂ in Ningbo Port, and 10.61% (6.96 µg/m³) to PM_{2.5} in Shanghai Port, respectively, regions with dense ship traffic. The relative differences in the PM_{2.5}, SO₂, and NO₂ concentrations modeled using monthly and hourly ship emissions accounted for -10–15%, -10–30%, and -5–30%, respectively. Compared with cruise- and land-based measurements, the simulations using hourly emissions were in much better agreement with the observations than those using monthly emissions and appropriately captured some air pollutant concentration peaks. Simulations during shipping-related periods with hourly ship emissions improved the normalized mean bias (NMBs) from -43.03%, 301.49%, and

* Correspondence to: Y. Zhang, Shanghai Institute of Eco-Chongming (SIEC), Shanghai 200062, China.

** Corresponding author.

E-mail addresses: yan_zhang@fudan.edu.cn (Y. Zhang), lmchen@fudan.edu.cn (L. Chen).

223.02% to -27.28% , 90.45%, and 167.52%, respectively, for $\text{PM}_{2.5}$, SO_2 , and NO_2 , highlighting the importance of using ship emissions with a fine temporal resolution. Our study showed that ignoring hourly fluctuations in ship emissions during air quality modeling leads to considerable uncertainties, especially in coastal urban areas and harbors with high ship activities. These results imply that data with a high temporal resolution, such as hourly ship emissions, are necessary to understand the realistic impacts of shipping traffic and to implement more precise control policies to improve coastal air quality.

© 2020 Elsevier B.V. All rights reserved.

1. Introduction

Ship emissions have become an increasingly important anthropogenic emission source, especially in coastal regions, and thus have become the subject of increasing concern in recent years (Corbett and Fischbeck, 1997; Capaldo et al., 1999; Cooper, 2003; Eyring et al., 2005; Sofiev et al., 2018). The key air pollutants in ship exhaust, including SO_x , NO_x , particulate matter (PM), and HC, play significant roles in air quality, weather, climate change, and human health (Lawrence and Crutzen, 1999; Eyring et al., 2010; Liu et al., 2016a; Thornton et al., 2017; Li et al., 2018). The global annual ship emissions of NO_x , SO_2 and $\text{PM}_{2.5}$ in 2015 were estimated to be 2×10^7 , 9.7×10^6 and 1.5×10^6 tons, respectively (Johansson et al., 2017). Corbett et al., (1999) showed that NO_x emissions from ships can account for much more than 10% of the total global anthropogenic NO_x emissions, and subsequent studies (e.g., Corbett and Koehler, 2003; Eyring et al., 2010) reported that the NO_x emissions of ships represented 15–30% of all global NO_x emissions. Liu et al., (2016a) indicated that ship-related NO_x emissions over East Asia reached 2.8 Tg in 2013, which was double the value in 2001, and Marelle et al. (2016) illustrated that ship emissions enhanced the concentrations of NO_x and SO_2 by 80% in the coastal area of Norway, leading to a decrease of 9.3 mWm^{-2} in total shortwave radiation. More recently, Thornton et al. (2017) demonstrated that aerosol particles and NO_x from ships affect maritime convection and enhance lightning over shipping lanes.

China, which has three high-intensity port clusters in the Pearl River Delta, Yangtze River Delta (YRD) and Bohai Rim, occupies an increasingly important proportion of global shipping, with trade contacts being formed frequently between China and other countries globally. Seven of the container ports in China ranked among the top ten container ports worldwide in 2016 (UNCTAD, 2017). The YRD, which is one of the busiest port clusters in China, comprises over 15 ports, including Shanghai Port, which has developed into the largest container port in the world since 2010, Ningbo-Zhoushan Port, Nantong Port, and Lianxing Port, resulting in high emissions of ship-related air pollutants in this region (Fan et al., 2016; Liu et al., 2016b). In an analysis of aerosol samples at Shanghai Port, Zhao et al. (2013) reported that ship traffic emitted $\text{PM}_{2.5}$ concentrations ranging from 0.63 to $3.58 \mu\text{g m}^{-3}$, accounting for 4.2% to 12.8% of the total $\text{PM}_{2.5}$ in the area, while Wang et al. (2019) recently estimated that ship emissions in Shanghai Port contributed 36.4%, 0.7%, 5.1%, -0.9% , and 5.9% of SO_2 , NO , NO_2 , O_3 , and $\text{PM}_{2.5}$, respectively, from combined land and ship sources in the summer of 2016.

A large number of studies, including land-based, ship-based and airborne measurements and model simulations (e.g., the Weather Research and Forecasting (WRF)-Chem model, the WRF-Community Multiscale Air Quality (CMAQ) model, and the Goddard Earth Observing System (GEOS)-Chem model), have been carried out to investigate the influences of ship emissions on air quality. To the best of our knowledge, ground observations can be used to investigate only the impacts of ship emissions at target locations, and the complexity of particle components, precursors and chemical reactions preclude the application of this method to the evaluation of secondary particles (Heo et al., 2017). Hence, air quality models are usually employed to estimate the impacts of ship emissions. Ding et al. (2018) employed satellite-derived ship emission data in a regional chemical transport model (CTM) and

concluded that the contribution of ship emissions to NO_x reached up to 20% along the coastline of the Pearl River Delta in summer. Chen et al. (2019) employed a WRF-Chem simulation to show that ship traffic sources contributed 4.0% to the annual $\text{PM}_{2.5}$ over the YRD in 2014, and Feng et al. (2019) reported that ships contributed $0.55 \mu\text{g m}^{-3}$ and $0.36 \mu\text{g m}^{-3}$ (January) and $0.73 \mu\text{g m}^{-3}$ and $0.75 \mu\text{g m}^{-3}$ (June) to the land ambient SO_2 and $\text{PM}_{2.5}$, respectively, based on WRF-CMAQ simulations.

Over the past few decades, numerous inventories providing ship emission distributions at high spatial resolutions have been developed. Fan et al. (2016) calculated ship emissions with a spatial resolution of $1 \text{ km} \times 1 \text{ km}$ at monthly and yearly time scales, and Chen et al. (2017a) developed a national ship emission inventory with a resolution of $0.005^\circ \times 0.005^\circ$ for 2014. In addition to the spatial resolution, the temporal resolution is also important for modeling simulations, especially for conducting comparisons with increasingly accurate time observations, for example, the measurements carried out in the East China Sea during June 2017 (Tan et al., 2018). de Meij et al. (2006) showed that NO_x and NH_3 emissions with high temporal and spatial resolutions are crucial for performing aerosol simulations, while Gilliland et al. (2003) reported that the results can be improved with a high spatiotemporal resolution, even without seasonal functions and diurnal variations. Chen et al. (2017b, 2018) applied yearly ship emissions to study the impacts of ship emissions on the air quality in Qingdao Port and the YRD. Lv et al. (2018) employed WRF-CMAQ data based on monthly ship emissions to research the impacts of ship emissions on $\text{PM}_{2.5}$ in China. Karl et al. (2019) used the Ship Traffic Emission Assessment Model (STEAM) with a resolution of $2 \text{ km} \times 2 \text{ km}$ and hourly updated ship emissions to evaluate the impact of emissions on the air quality in the Baltic Sea with different regional chemistry models. Most of the abovementioned studies did not analyze the uncertainties associated with monthly or average emissions.

Nevertheless, many studies have reported that the contributions of ship emissions to the air quality over harbors and coastal cities are confined to a limited distance. For example, Poplawski et al. (2011) found that the majority of contributions from cruise ship emissions in Victoria's port, Canada, is limited to approximately 1 km from the mooring points, whereas these contributions can reach up to 5 km inland at Taranto, Italy (Gariazzo et al., 2007). Chen et al. (2018) estimated that the highest impact of $\text{PM}_{2.5}$ is emitted by ships up to 10 km from the coastline in the Bohai Rim region in China. Liu et al., (2016b) indicated that ships could contribute up to 20–30% of the total $\text{PM}_{2.5}$ during periods influenced by ship plumes and approximately 11% 10 km from the coastline. Since ship plumes are very dynamic due to the nature of mobile sources, on-line high temporal resolution observations also reflect the strong time dependence of the contribution of ship emissions (Liu et al., 2016b, Zhang et al., 2019). Thus, it is important to determine the distributions of ship emissions at high spatial and temporal scales to accurately assess the influence of ship exhaust on coastal air quality. Although some researchers have used ship emissions at high spatial and temporal resolutions to simulate environmental impacts and have compared the simulation results with measurements for given periods (Liu et al., 2016b) and recommended that spatially gridded ship emissions with hourly resolution are used modeling simulations based on modeled the spatial extent of different temporal emissions using regression analysis (Goldsworthy et al., 2019), few investigations have used

regional online measurements in coastal zones with busy traffic activities to evaluate fine-resolution simulation results and verify the importance of a finer emissions inventory for air quality modeling in busy ship traffic regions relative to average emission inventories. Consequently, the limitations and uncertainties of annual and monthly ship emissions in simulating coastal air quality are unresolved.

This study aimed to evaluate the importance of the temporal resolution of ship emission data in modeling air quality by taking the coastal YRD, one of the busiest ship traffic regions worldwide, as an example. The modeling results based on ship emission data with different temporal resolutions were systematically evaluated by both cruise measurements and land-based observations at nearby port sites in Shanghai and Ningbo.

2. Study area, data and methods

2.1. Air quality model setup and configuration

The study area spanned the region from 29°N to 34°N and from 117.5°E to 123.8°E, covering all ports in Yancheng, Nantong, Shanghai, Hangzhou, and Ningbo-Zhoushan (Fig. 1a). We employed a regional multiscale meteorology and online chemistry model, WRF-Chem (version 3.7.1) (Grell et al., 2005), to evaluate the temporal resolution of ship emissions. The key model configurations in the present study were the same as those in Mao et al. (2018). The initial and boundary conditions for the meteorology were generated from the National Centers for Environmental Prediction (NCEP) Final (FNL) global reanalysis data with a horizontal resolution and time interval of 1° × 1° and 6 h, respectively. The detailed anthropogenic emissions (land-based and ship sources) are described in Section 2.2, while biogenic emissions, which were also taken into consideration, were calculated online using the Model of Emissions of Gases and Aerosols from Nature (MEGAN) (Guenther et al., 2006).

WRF-Chem was used to perform three nested domain simulations with horizontal resolutions of 81, 27, and 9 km (see Fig. 1 in Mao et al., 2018) and a vertical resolution of 22 layers (from the surface to ~11.8 km) with 8 levels below 1.5 km. Domain 1 covered East Asia and part of Southeast Asia, while nested domains 2 and 3 covered a large part of East China and the YRD (including Zhejiang, Shanghai and Jiangsu Provinces), respectively.

Three separate simulations were conducted in the present study: (1) only land-based emissions (OLDE), (2) land-based emissions with

monthly (June 2017) ship emissions (LMSE), and (3) land-based emissions with hourly ship emissions (LHSE). Our simulations covered the period from 2 to 29 June 2017, during which continuous measurements were acquired, with a 3-day spin-up time.

2.2. Emission inventory

2.2.1. Hourly ship emissions

Bottom-up ship emissions, which were collected onboard to record real-time activity information, were derived from automatic identification system (AIS) data, and the emission inventory estimation followed the AIS-based methodology detailed in Fan et al. (2016) and Feng et al. (2019). In this study, both monthly ship emissions (June 2017) and refined (hourly) ship emissions were estimated to investigate the impacts of ship emissions on coastal air quality simulations at different temporal scales. SO₂, NOx, NH₃, CH₄, non-methane volatile organic compounds (NMVOCs, hereafter simply VOCs), CO, CO₂, PM_{2.5}, PM₁₀, black carbon (BC), and organic carbon (OC) were included in our ship emission inventory. Notably, the hourly profiles of 17 and 18 June came from the average hourly AIS data from 1 to 16 and from 19 to 30 June (28 days) and the real-time AIS data from the Shanghai Maritime Safety Administration, respectively, since AIS data were missing for these two days in the original database. We recognize that there are some uncertainties associated with these hourly ship emissions due to the lack of records for some days in the AIS database. However, the fine hourly resolution of the ship emission inventory represents a first attempt that, as shown below, improved the modeling skill in simulating the concentrations of pollutants emitted by frequently moving vessels.

2.2.2. Non-ship emissions

For the land-based anthropogenic sources in 2015, yearly particulate and gas emissions for Asia, except for mainland China, were derived from the International Institute for Applied Systems Analysis (IIASA) database with SO₂, NOx, CO, VOCs, PM₁₀, PM_{2.5}, NH₃, primary BC and OC data included at a 0.5° × 0.5° horizontal resolution (Stohl et al., 2015). In contrast, the emissions for mainland China were obtained from Tsinghua University and included SO₂, NOx, VOCs, PM₁₀, PM_{2.5}, and primary BC and OC with a 27 km × 27 km horizontal resolution (without NH₃ and CO) (Zhao et al., 2018). NH₃ and CO emissions for mainland China were obtained from the IIASA database. We employed a more refined emission inventory developed by the Shanghai Academy of Environmental Sciences (SAES) with a 4 km × 4 km resolution for 2014 for

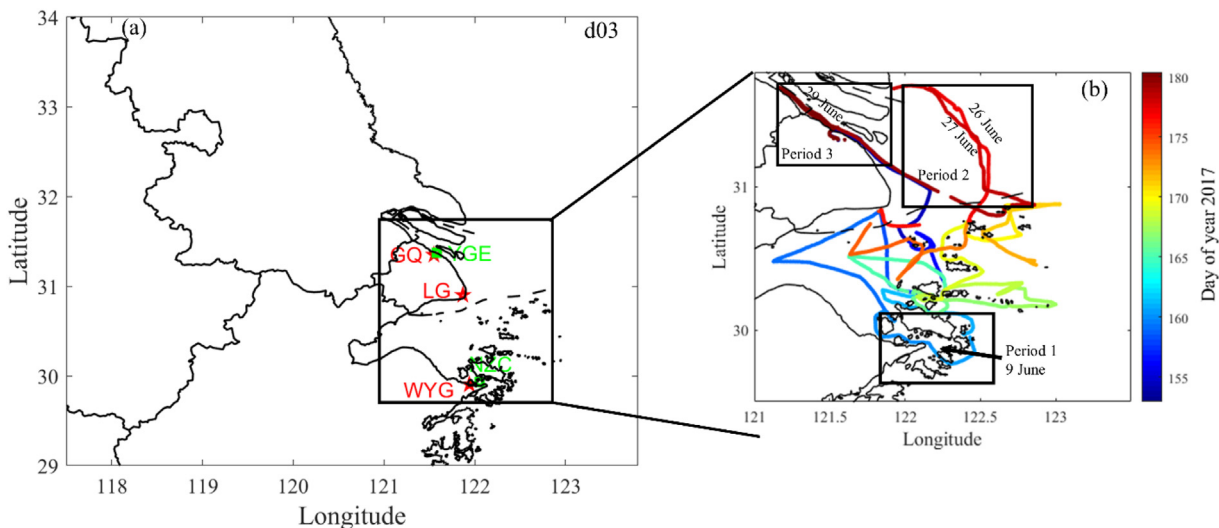


Fig. 1. (a) Nested domain 3 covers all ports in Yancheng, Nantong, Shanghai, Hangzhou, and Ningbo-Zhoushan with coastal sites and source area samples positioned, (b) The ship-based measurement campaign cruise and three periods in high polluted areas along shipping cruise route. Pentagram and square in (a) represent coastal sites (GQ: Gaoqiao, Shanghai; LG: Lingang, Shanghai; WYG: Wenyiguan, Ningbo) and source area samples (YGE: Yangtze Estuary nearby Waigaoqiao port; NZC: Ningbo-Zhoushan channel). The ship cruise in (b) is colour coded by the observed JULIAN days.

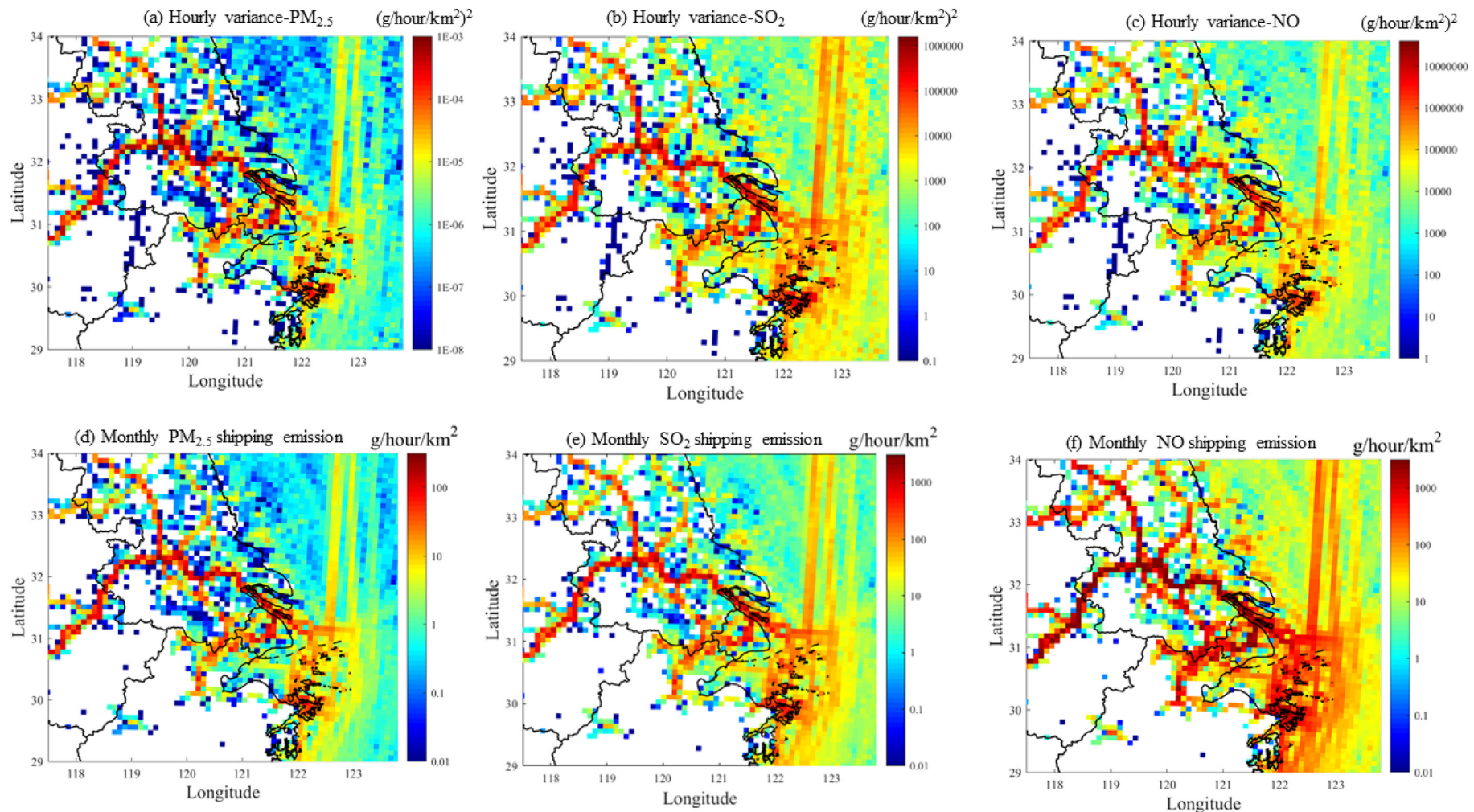


Fig. 2. The hourly variance between monthly mean and hourly (a) PM_{2.5} emissions, (b) SO₂ emissions, and (c) NO emissions and horizontal distributions of monthly mean (d) PM_{2.5} emissions, (e) SO₂ emissions, and (f) NO emissions. The calculation of hourly variance follows the formula: hourly variance(i) = $\frac{\sum (E_{ih} - E_{im})^2}{N}$, i represents pollutant species; E_{ih} and E_{im} represent hourly and monthly average emission flux of species i, and N represents total hours of June.

the YRD. The hourly variations followed the profiles described in Tan et al., 2015, and ArcGIS (version 10.2, ESRI: ArcGIS 10.2, 2013) was used to allocate area and stack sources into grids in the emission inventory. Notably, the emission inventory in this study contained data on ship emissions distributed across the surface layer. More detailed descriptions of the land-based emission inventory are given in Mao et al. (2018) and Feng et al. (2019).

2.3. Ship cruise and land-based measurement data

The cruise- and land- based observational data were used to evaluate the simulation results in this study. The ship-based measurement campaign was carried out in the East China Sea, including the Yangtze Estuary and coastline of the YRD, from 2 to 29 June 2017 (Fig. 1b). The ship departed from Gongqing Port, Shanghai, on 2 June and returned to Gongqing Port on 29 June by way of Yangshan Port, the Ningbo-Zhoushan channel, Lianxing Port of Qidong, Jiangsu Province, Huaniao Island, and the Yangtze Estuary. The measurements related to this study, including the wind speed and wind direction data, were recorded by a Vaisala Automatic Weather Station AWS310, and ground concentrations of NO₂, SO₂, and PM_{2.5} were monitored by Thermo i-Series analyzers (42i for NO₂, 43i for SO₂, and 5030i for PM_{2.5}). Additionally, the vertical column densities (VCDs) of NO₂ and SO₂ were measured by multiaxis differential optical absorption spectroscopy (MAX-DOAS) with a temporal resolution of 4 min along cruise tracks were used to evaluate the simulated vertical concentrations of air pollutants; the observational detailed information is given by Tan et al. (2018). Furthermore, the hourly SO₂ data measured by a Thermo 43i analyzer at coastal inland sites including the Gaoqiao (Shanghai), Lingang (Shanghai), and Wenyiguan (Ningbo) sites were employed to evaluate simulation results in inland regions influenced by ship emissions (Fig. 1a).

3. Results

3.1. Characteristics and dynamics of ship emissions in the YRD

The total emissions of PM_{2.5}, SO₂, and NOx from ships in June 2017 estimated based on the AIS data over the YRD were 1.3×10^3 t, 9.3×10^3 t, and 3.7×10^4 t, respectively, which are comparable to the reports of previous studies.

Fig. 2 shows the hourly variance between the hourly and monthly mean PM_{2.5}, SO₂, and NO emissions (Fig. 2a–c) and the horizontal distributions of the monthly mean PM_{2.5}, SO₂, and NO emissions (Fig. 2d–f). Clearly, the variations in the spatial distributions of PM_{2.5}, SO₂, and

NOx (Fig. 2a–c) were similar to the emission fluxes (Fig. 2d–f), especially at Shanghai Port, the Yangtze Estuary and the Ningbo-Zhoushan channel, and large discrepancies were detected, except for inland waters. The Yangtze Estuary near Waigaoqiao Port, northeastern Shanghai, the largest port in China (Wang et al., 2019), and the Ningbo-Zhoushan channel, which is surrounded by the Zhoushan Islands, are both stops located on busy shipping lanes; thus, these ports were chosen to illustrate the large discrepancies in the hourly and monthly mean data. Fig. 3 compares the hourly SO₂ emission fluxes in June 2017 with the hourly mean SO₂ emission fluxes in the monthly inventory for the Yangtze Estuary and Ningbo-Zhoushan channel (locations shown in Fig. 1a). The hourly ship emissions showed clear diurnal variations. In the Yangtze Estuary, the hourly ship emission fluxes ranged from 0 to 2915.93 g/h/km² (1082.41 ± 444.41 g/h/km²), while the monthly ship emissions were constant at 1082.41 g/h/km². Similarly, the maximum and minimum emissions fluxes varied from 0 to 3802.52 g/h/km² (593.55 ± 404.95 g/h/km²), while the monthly ship emissions were an invariant 593.55 g/h/km² in the Ningbo-Zhoushan channel, which contains the largest container throughput port in the world. Thus, these simulations of models using monthly ship emissions yielded over- or underestimations regardless of hourly fluctuations in the ship emission inventory. To evaluate the effects of different temporal resolutions of ship emissions, comparisons of the simulations based on the monthly and hourly ship emission data with the measurements collected during 2–29 June 2017 along a ship cruise route and at various coastal inland sites are discussed in the next sections.

3.2. Impacts of ship emissions on air quality in the YRD by modeling

3.2.1. Contributions of ship emissions to air quality based on monthly ship emissions (LMSE)

Fig. 4 shows spatial distributions of simulated surface SO₂, NO₂, and PM_{2.5} concentrations (left panels) and the absolute (middle panels) and relative (right panels) contributions of monthly ship emissions to the simulated surface SO₂, NO₂, and PM_{2.5} concentrations in the YRD. Fig. 4a, d, and g depict the monthly mean concentrations of SO₂, NO₂ and PM_{2.5} by LMSE, with ranges of 3–15 ppbv, 5–25 ppbv, and 20–120 µg/m³, respectively, over the continent and low pollutants over the oceans. For all pollutants, except for some hot spots caused by industrial emissions, high concentrations were distributed mainly along inland shipping lanes, such as the Yangtze River and Huangpu River, highlighting the dominant impact of ship emissions on the air quality of coastal cities in summer. The results clearly reveal that the influences of ship emissions on SO₂ and NO₂ are confined primarily to

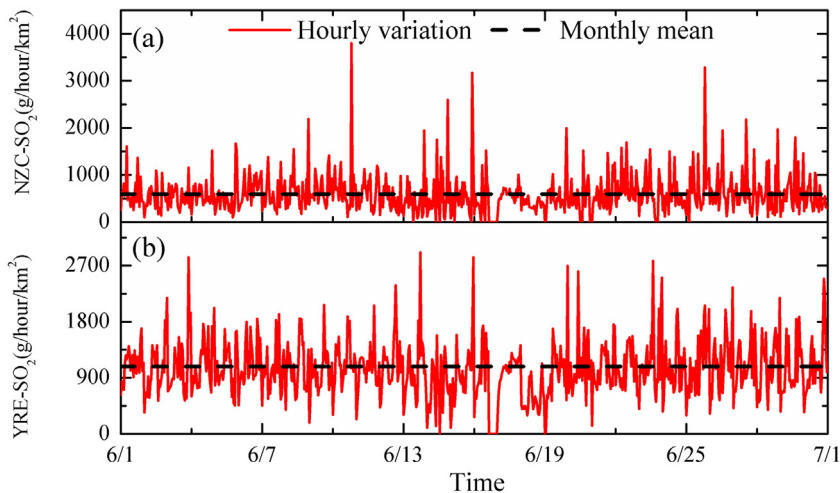


Fig. 3. Time series of hourly SO₂ emission fluxes in June 2017 with the monthly mean SO₂ emission in monthly inventory located in (a) Ningbo-Zhoushan and (b) Yangtze River Estuary. Red lines represent the hour by hour ship emission fluxes, and black dash lines represent monthly average based on hourly ship emission fluxes.

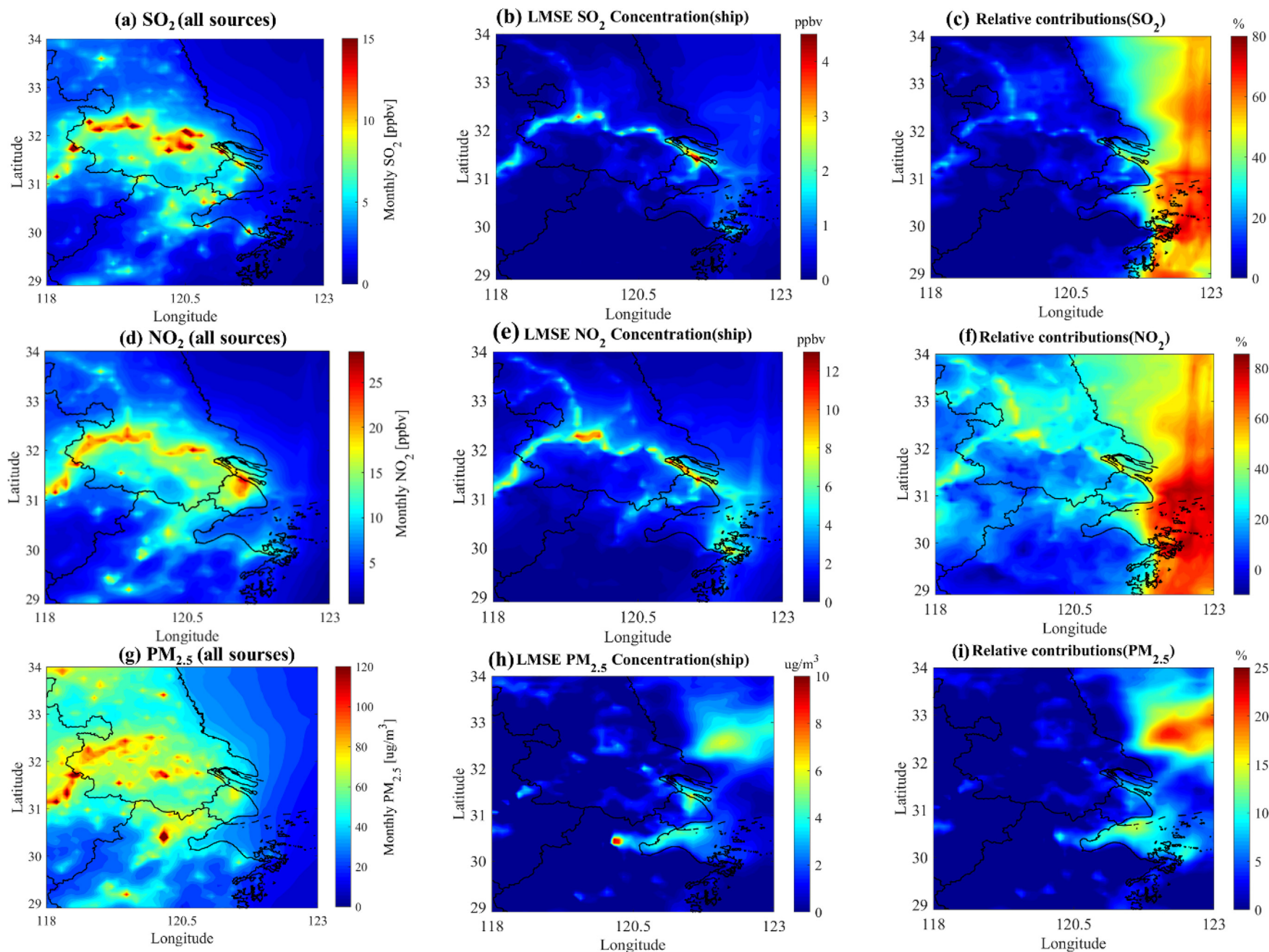


Fig. 4. Spatial distributions of simulated surface SO₂, NO₂, and PM_{2.5} concentrations using monthly ship emissions (left panels), absolute (LMSE-OLDE, middle panels) and relative ((LMSE-OLDE)/LMSE, right panels) contributions of monthly ship emissions to the simulated surface SO₂, NO₂, and PM_{2.5} concentrations in the YRD.

nearby ship lanes (Fig. 4b and e). Ship emissions contributed anywhere from 0 to 4 ppbv (~5–40%) and from 0 to 14 ppbv (0–80%) to the monthly mean values of SO₂ and NO₂ over land, respectively, and the contributions to SO₂ and NO₂ ranged mainly from 0.5 to 4 ppbv (~5–40%) and from 1 to 8 ppbv (~10–35%), respectively, in urban Shanghai. Compared with the contributions to SO₂ and NO₂, inland vessels contributed less to terrestrial PM_{2.5}, with contributions mainly below 3 $\mu\text{g}/\text{m}^3$ (<8%). High impacts were detected in Shanghai with a contribution range of 1–5 $\mu\text{g}/\text{m}^3$, and the highest relative contribution reached ~11%. Fig. 4h and i also clearly show that a hotspot for PM_{2.5} occurred in Hangzhou urban area, with concentration up to 9 $\mu\text{g}/\text{m}^3$ (11%). In particular, ships contributed significantly to the SO₂, NO₂, and PM_{2.5} concentrations in Shanghai Port and Ningbo Port, reaching 6.64 ppbv, 13.92 ppbv, and 6.96 $\mu\text{g}/\text{m}^3$ (54.47%, 52.0% and 10.61% of PM_{2.5} by LMSE), respectively, in Shanghai Port and 2.15 ppbv, 8.79 ppbv, and 0.28 $\mu\text{g}/\text{m}^3$ (80.72%, 81.79%, and 1.51% of SO₂, NO₂, and PM_{2.5} by LMSE), respectively, in Ningbo Port. These results for SO₂ and NO₂ demonstrate that the maximum absolute pollutant concentrations occurred in Shanghai Port, but Ningbo Port had the highest contributions of shipping emissions relative to ambient pollutants, while both absolute and relative peaks of PM_{2.5} were in Shanghai Port. Moreover, the contributions of ship emissions to the maximum daily mean SO₂, NO₂, and PM_{2.5} were in the ranges of 0.5–7 ppbv (~5–40%), 2–15 ppbv (~8–40%), and 4–60 $\mu\text{g}/\text{m}^3$ (~5–40%), respectively, in urban Shanghai, and ship emissions accounted for ~20–45% (~20–80 $\mu\text{g}/\text{m}^3$) in the maximum daily mean PM_{2.5} along the coastline of Jiaxing, Hangzhou, and Ningbo, Zhejiang Province (Fig. S1). The results based on monthly emission inventory show clearly that the influence of ship emissions on SO₂ and NO₂ mainly confined to nearby ship lanes, also the higher impact of

PM_{2.5} occurred in port nearby region, which implied the importance of high resolution ship emissions around ship lanes.

3.2.2. Differences in simulating air quality caused by the shift to hourly ship emissions (LHSE)

The contribution of hourly ship emissions (LHSE), the absolute differences (LHSE-LMSE) and the relative discrepancies (LHSE-LMSE)/LMSE of PM_{2.5}, SO₂ and NO₂ were presented in Fig. 5. Overall, the contributions of hourly ship emissions to all pollutants (PM_{2.5}, SO₂, and NO₂) were lower than those of monthly ship emissions in inland rivers (e.g., the Changjiang River and Huangpu River) and significantly higher in the nearby Ningbo-Zhoushan channel (Fig. 5a, d, and g). For SO₂, the main differences in the surface concentrations were distributed along shipping lanes and the coastline, and the differences between the LHSE and LMSE were in the ranges of ~20–30% over the ocean and ~10–25% on the coast, where the Ningbo-Zhoushan channel exhibited the maximum difference, with a range of ~20–25% (~0.2–0.4 ppbv) and contributions of ships decreased from ~2% to 7% (~0.1–0.6 ppbv) in northern Shanghai (Fig. 5b–c). In addition, ship emissions affected the SO₂ concentrations of inland Ningbo. Similarly, Fig. 5e and f illustrate that high values of surface NO₂ were generally confined to shipping lanes, and NO₂ concentrations predicted using LHSE were ~25–40% (~0.5–1.5 ppbv) higher than those using LMSE along the coastline near Jiangsu, ~5–30% (~0.5–1.5 ppbv) overestimated in the Ningbo-Zhoushan channel and ~5–30% (~0.5–1.5 ppbv) underestimated in near Shanghai downtown and Shanghai Port, with overestimated values ranging from 20% to 65% over the ocean. Fig. 5 h and i show that the PM_{2.5} contribution in the Ningbo-Zhoushan channel modeled using LHSE was approximately 10–15% (~2–3 $\mu\text{g}/\text{m}^3$) higher

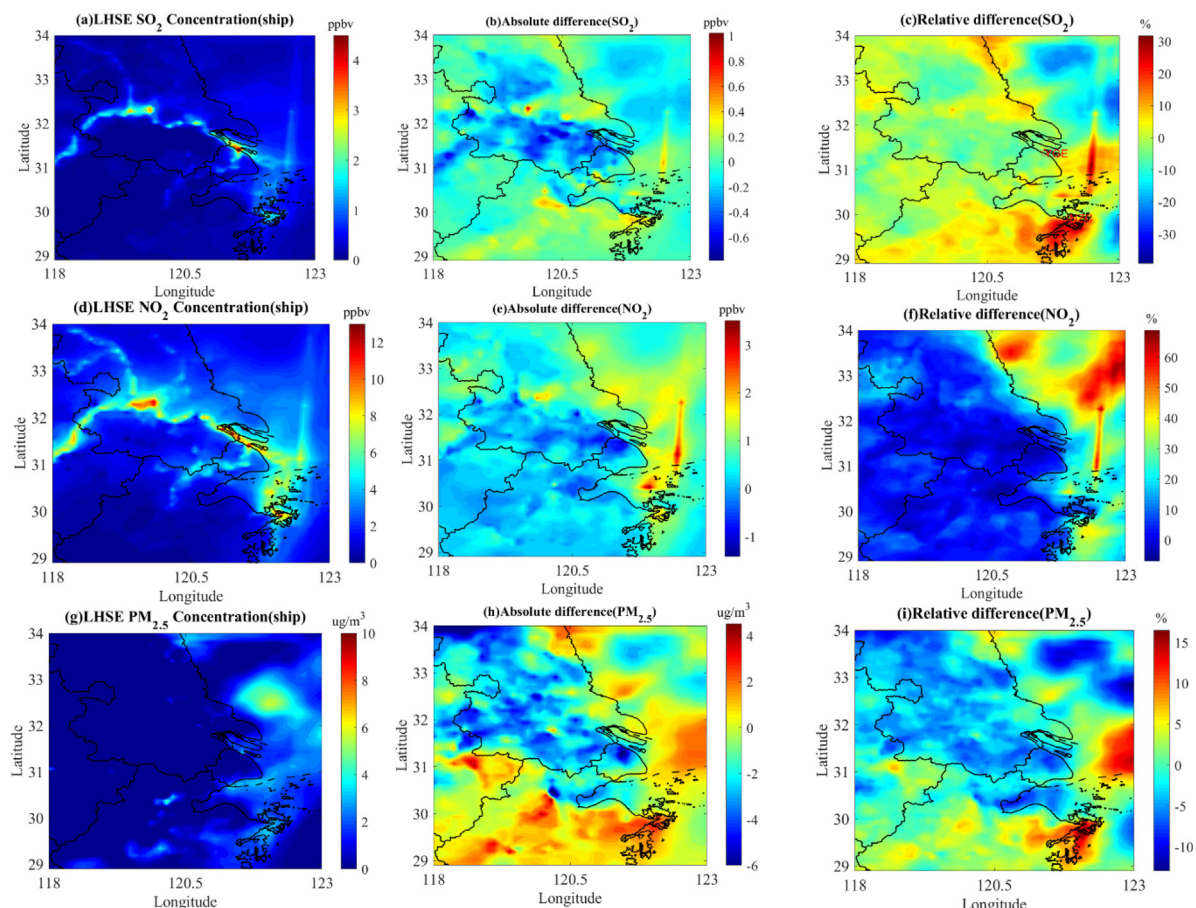


Fig. 5. Contributions of hourly ship emissions on SO₂, NO₂, and PM_{2.5} concentrations (LHSE-OLDE, left panels), absolute (LHSE-LMSE, middle panels) and relative ((LHSE-LMSE)/LMSE, right panels) discrepancies of SO₂, NO₂, and PM_{2.5} between LMSE and LHSE.

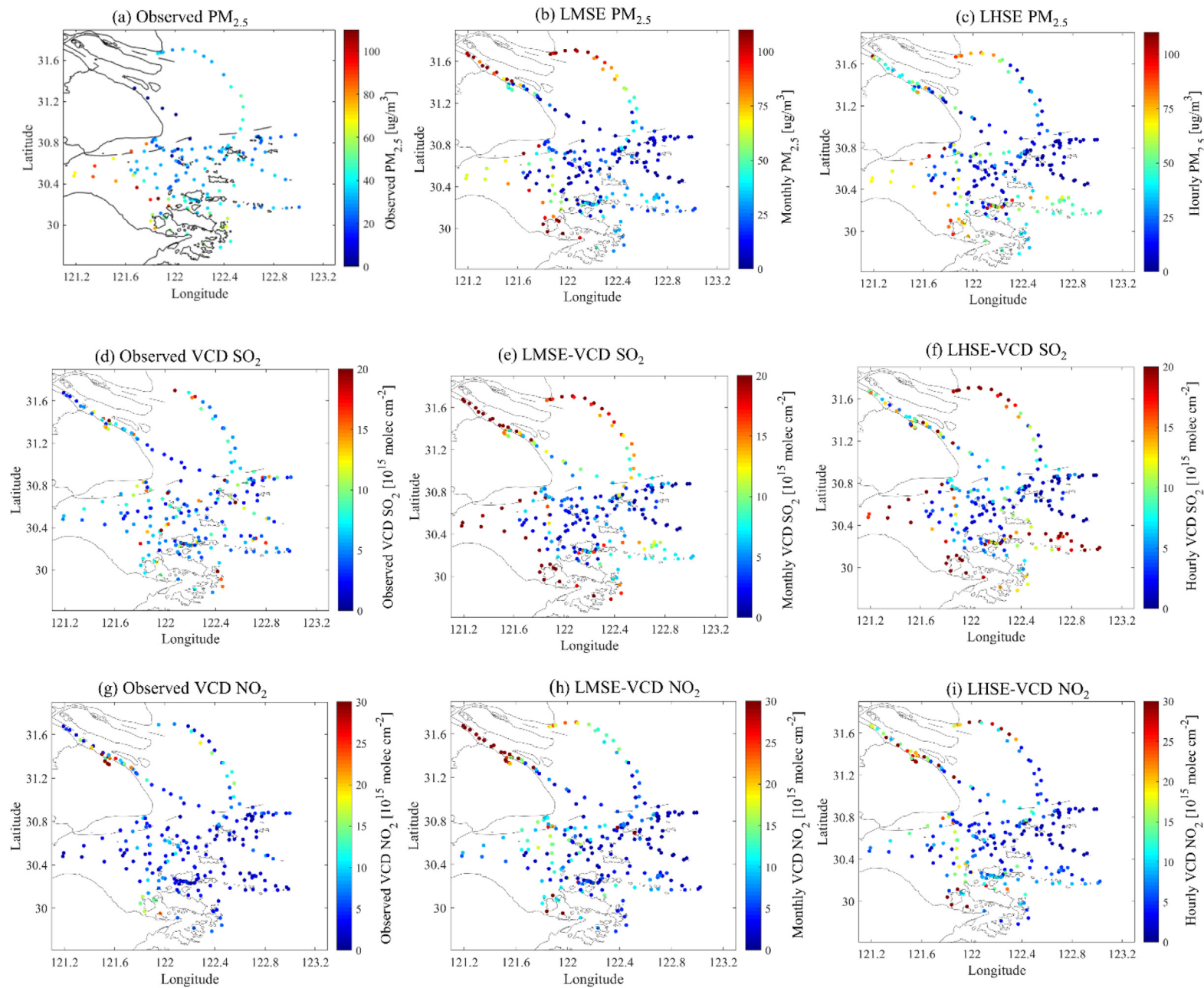


Fig. 6. Spatial distributions of observed concentrations of (a) surface PM_{2.5}, (d) column SO₂, (g) column NO₂, and simulated concentrations of (b) surface PM_{2.5}, (e) column SO₂, (h) column NO₂ by monthly (June 2017) ship emission (LMSE) and (c) surface PM_{2.5} (f) column SO₂, (i) column NO₂ by hourly ship emission (LHSE) along ship cruise. The surface PM_{2.5} concentrations were observed by cruise-based Thermo 5030i, and the column concentrations of SO₂ and NO₂ were observed by cruise-based DOAS.

than that modeled using LMSE, accounting for the highest values over the coastline along the YRD; $\text{PM}_{2.5}$ was underpredicted by ~5%–10% ($\sim 2\text{--}6 \mu\text{g}/\text{m}^3$) in Shanghai downtown and Shanghai Port, by ~2%–7% ($\sim 1\text{--}5 \mu\text{g}/\text{m}^3$) along the coastline of Jiaxing and Ningbo, and by less than ~6% ($\sim 4 \mu\text{g}/\text{m}^3$) in inland Jiangsu Province, while ship emissions modeled using LHSE were more than 10% greater than those modeled using LMSE in the remote ocean of eastern Shanghai. For the concentrations of all pollutants ($\text{PM}_{2.5}$, SO_2 , and NO_2), the contributions of ships using the hourly emission inventory clearly decreased in Shanghai Port but increased in the Ningbo-Zhoushan channel and along the coastline of Jiangsu Province compared with those using the monthly emission inventory, and the most significant differences between the two ship emission inventories occurred at harbors with frequent activities, such as Shanghai Port and the Ningbo-Zhoushan channel, and over the remote oceans as a result of clear variations in the hourly emission intensity (Fig. 3).

3.3. Importance of high-resolution ship emissions in simulating the air quality of coastal areas evaluated by measurements

3.3.1. Comparisons of modeling results with cruise measurements in coastal sea regions

Fig. 6a, b and Fig. S2 compare the surface concentrations of $\text{PM}_{2.5}$, SO_2 , and NO_x by LMSE with ship-based measurements along the cruise route shown in Fig. 1b. The modeling simulations captured the spatial changes in $\text{PM}_{2.5}$, NO_2 , and SO_2 during the measurements. Additionally, all pollutant concentrations were greatly overestimated in harbor areas, including the Yangtze Estuary, Shanghai Port, the Ningbo-Zhoushan channel, and Lianxing Port (located nearby in Qidong); this overestimation was especially notable in the Yangtze Estuary and Shanghai Port, which have some of the highest vessel activities in China.

Ship exhaust is emitted from funnels dozens of meters above the ship deck; this physical configuration leads to the difficulty in measuring the impacts of ship emissions on air quality in the real atmosphere and overestimations compared with ground observations (a few meters above ground) because ship emissions are allocated throughout the surface layer (from the surface to 50 m above the surface) in emission inventories. Hence, in this study, it seemed reasonable to compare the simulated column concentrations with the observed VCDs of NO_2 and SO_2 reported by Tan et al. (2018). The results indicate that column concentrations were much more comparable than were the surface concentrations in evaluations of the modeling performance. **Fig. 6d, e, g, and h** exhibit the spatial distributions of the observed and simulated column concentrations of SO_2 and NO_2 by LMSE along the ship cruise route. Along the cruise route, the simulated column concentrations of SO_2 were in the range of 5.67×10^{13} to $5.54 \times 10^{16} \text{ mol cm}^{-2}$, and the measured VCDs ranged from 1.31×10^{15} to $4.01 \times 10^{16} \text{ mol cm}^{-2}$ (**Fig. 6d** and e). The column concentrations of NO_2 varied from 4.51×10^{14} to $9.51 \times 10^{16} \text{ molec cm}^{-2}$, while the observed VCDs ranged from 4.28×10^{14} to $4.37 \times 10^{16} \text{ mol cm}^{-2}$ (**Fig. 6g** and h). The model captured some high values of the SO_2 VCDs but overall overestimated them. The simulated VCDs of NO_2 were better than the calculated

surface concentrations of NO_2 . The mean values and normalized mean biases (NMBs) are summarized in Table 1 to show the performance of the simulated $\text{PM}_{2.5}$, SO_2 , and NO_2 , revealing that the model overestimated the average concentrations of SO_2 and NO_2 with NMBs of 82.74% and 30.94%, respectively, while the mean concentration of $\text{PM}_{2.5}$ was underestimated (NMB = -26.82%). The NMBs of the column concentrations of NO_2 and SO_2 are shown in Table 1, showing values of 55.40% and 18.29%, respectively.

The simulated surface and column concentrations of the pollutants in harbor areas were both much higher than the observations. The reasons for these large differences may include but are not limited to uncertainties in the emission inventories, such as estimations of emission factors and monthly accumulated ship emissions, meteorology, photolysis chemistry, and measurements. For these reasons, the monthly ship emissions without hourly variations could not accurately reproduce the fluctuations of the pollutants, reflecting the considerable importance of ship emissions with a refined (hourly) temporal resolution in modeling simulations.

As shown above, the modeled column concentrations were more realistic than the surface measurements of tracer gases (NO_2 and SO_2) in the present study, so we focused predominantly on the column differences using hourly ship emissions compared with the observed VCDs of NO_2 and SO_2 , while $\text{PM}_{2.5}$ was shown to present a change trend in the surface concentrations.

Fig. 6c, f, and i show the simulated surface concentrations of $\text{PM}_{2.5}$ and the column concentrations of NO_2 and SO_2 along the cruise route simulated by LHSE. Compared with the simulated $\text{PM}_{2.5}$ and NO_2 shown with monthly ship emissions without 24-h variations in **Fig. 6b** and S2d, there was a significant improvement in the simulations and change trend with a change in longitude (**Fig. 6c** and i) in Shanghai Port for both $\text{PM}_{2.5}$ and NO_2 ; however, the NMB of $\text{PM}_{2.5}$ was -32.91%, reflecting substantial underestimation (**Fig. S3a**), and that of NO_2 was 60.21%, which was far overestimated (**Fig. S3c**) relative to the results using monthly ship emissions. For SO_2 , the simulated values were in much better agreement with the measured VCDs (NMB of 8.35%) than the modeled results using monthly ship emissions, which were much more in accordance with the observations (**Fig. S3b**); in particular, the values dramatically decreased in Shanghai Port and were consistent with the observations. There was also an obvious improvement in the simulated $\text{PM}_{2.5}$ in the Ningbo-Zhoushan channel and the nearby waters of Qidong, which are highly polluted harbor areas, but NO_2 and SO_2 were overestimated in these regions by the simulations using monthly emissions.

To explore the impact of ship emissions on the simulations, we defined pollution with a contribution from ship traffic exceeding 60% as ship-related air pollution, whereas land-induced or land-ship-combined air pollution had a ship contribution of less than 60%. In addition, periods with differences between the observed and modeled wind directions within -30° to 30° were selected for further comparison. The results during these ship-related periods with hourly ship emissions were very consistent with the observations, with NMBs decreasing from -43.03%, 301.49%, and 223.02% to -27.28%, 90.45%, and 167.52% for $\text{PM}_{2.5}$, SO_2 , and NO_2 , respectively, highlighting the

Table 1

Statistical performance of simulated surface and column (values given in parentheses) concentrations of $\text{PM}_{2.5}$, NO_2 , and SO_2 using monthly shipping emissions along the ship cruise route in domain 3.

Variables	No. samples	Obs. ave	Sim. ave	NMB
$\text{PM}_{2.5}$	329	36.17	26.46	-26.82(-32.91)
SO_2	558(268)	1.59(7.35E+15)	2.91(8.7E+15, 7.97E+15)	82.74(18.29, 8.35)
NO_2	460(311)	6.62(5.93E+15)	8.67(9.20E+15, 9.50E+15)	30.94(55.40, 18.29)

Notes: the unit of Obs.ave. and Sim.ave. for $\text{PM}_{2.5}$: $\mu\text{g}/\text{m}^3$, the unit of Obs.ave. and Sim.ave. for SO_2 and NO_2 : molec cm^{-2} , the unit of Variations in normalized mean bias (NMBs): %. The simulated vertical column densities and NMBs in parentheses represent results by monthly and hourly ship emissions, respectively. The NMB of $\text{PM}_{2.5}$ in parentheses represents result by hourly ship emissions.

importance of using ship emissions with a fine temporal resolution, especially for SO₂. The simulations during the land-induced and land-ship-combined periods using hourly ship emissions performed slightly better than those using monthly ship emissions, except for PM_{2.5}. It should be noted that SO₂ and NO₂ were overestimated even using hourly ship emissions, indicating that the SO₂ and NO₂ emitted by ships may be widely overestimated. Another possible reason for the overestimation of NO₂ may be that the nonlinear chemistry of NOx is ignored in ship plumes.

3.3.2. Comparisons of modeling results with cruise measurements in coastal sea regions

To further investigate the differences between the monthly and hourly ship emissions in harbor areas, we selected three highly polluted areas in three periods, as shown in Fig. 1b. The measurements in period 1 on 9 June were carried out in Hangzhou Bay and the Zhoushan Islands. In period 2 from 26 to 27 June, the ship was entering and departing Qidong (Lianxing Port). In period 3 on 29 June, the ship arrived in Shanghai through the Yangtze Estuary.

Fig. 7 depicts comparisons of simulated surface concentrations of PM_{2.5}, column concentrations of SO₂, and NO₂ using hourly and monthly ship emissions with observations, and Table 2 gives the corresponding NMBs in the three periods shown in Fig. 1b. For PM_{2.5}, as shown in Fig. 7a, d, and g, the simulations using hourly ship emissions were most consistent with the observations in period 1 (Ningbo-Zhoushan channel) with NMBs of 0.93% (16.67% contribution of monthly ship emissions); in particular, the peak concentration simulated by LHSE (92.60 µg/m³) was closer to the observed peak value (76.94 µg/m³) at 11 am than that simulated (132.36 µg/m³) by LMSE. The PM_{2.5} values simulated using monthly ship emissions were in the best agreement with the observations from 1:00 to 11:00 AM on 26 June and were slightly less overestimated than the simulations employing monthly ship emissions overall based on the limited measurements in period 2. Compared with the observed SO₂ concentrations in these three periods, the simulated VCDs of SO₂ were highly overestimated by LMSE, especially for some peak values, such as the false peaks in period 1 of 5.15×10^{16} and 3.81×10^{16} molec cm⁻² estimated by LMSE and LHSE, respectively; in comparison, the observed value was 7.07×10^{15} molec cm⁻². Nevertheless, the simulations using hourly ship emissions yielded results relatively close to the measurements, particularly during period 3; the VCDs of SO₂ ranged from 2.59×10^{15} to 1.77×10^{16} molec cm⁻² by LHSE, with measured values ranging from 1.31×10^{15} to 1.60×10^{16} molec cm⁻², while the LMSE-modeled SO₂ varied from 9.62×10^{15} to 5.54×10^{16} molec cm⁻² (the NMBs decreased from 348.33% to 22.01%). For NO₂, both cases using hourly and monthly ship emissions captured the measured VCDs of NO₂ in period 1 with a simulated peak value (5.22×10^{16} molec cm⁻²) derived from hourly ship emissions that was slightly lower than that (5.91×10^{16} molec cm⁻²) derived from monthly ship emissions (the NMBs for the monthly and hourly ship emissions were 28.68% and 22.50%, respectively, during period 1). In period 2, the simulations using monthly ship emissions were in better agreement with the observations than were those using hourly emissions from 5:00 to 8:00 AM on 26 June, while the hourly ship emissions produced better results than the monthly ship emissions on 27 June. The column concentrations (2.08×10^{16} to 6.06×10^{16} molec cm⁻²) simulated using LMSE were much more overestimated than those (8.98×10^{16} to 4.03×10^{16} molec cm⁻²) simulated using LHSE in period 3 compared with the observations (1.49×10^{15} to 4.36×10^{16} molec cm⁻²), with NMBs of 185.13% (monthly) and 54.92% (hourly). Overall, the simulations using LHSE in harbor areas performed best, providing peak values that were decreased to levels closer to the actual measurements, especially for SO₂, which was significantly improved by using LHSE, highlighting the necessity of hourly ship emissions. Figs. 8 and S4 show the vertical profiles of PM_{2.5}, SO₂, and NO₂ during periods 1 (Ningbo-Zhoushan channel) and 3 (Yangtze Estuary). It is clear that all vertical concentrations

simulated using LHSE decreased overall compared to those simulated using LMSE, especially in period 3. The differences in the vertical distributions of all pollutants were further caused by horizontal transportation and vertical turbulence.

3.3.3. Comparisons of modeling results with measurements in coastal inland sites

To show the improvements resulting from the use of hourly ship emissions, coastal inland sites during periods affected by ships were chosen (shown in Fig. 1a); the sites were Wenyiguan and Gaoqiao, which are located along the routes of heavy shipping, and Lingang, which is in an area with little ship activity. Fig. 9 compares the SO₂ (primary pollutant) concentrations modeled by LMSE and LHSE with the observations at the Wenyiguan, Gaoqiao, and Lingang sites during the periods of 10–15 June, 19–24 June, and 23–29 June, respectively. At the sites with heavy ship emissions (Fig. 9a and b), the LHSE modeling captured some real peaks, while the LMSE modeling simulated false peaks. The false simulated peaks of 11.80 and 9.48 ppbv by LMSE were much higher than the observations (2.8 and 3.5 ppbv, respectively), while the SO₂ values modeled using LHSE were 3.0 and 2.01 ppbv at 11 am on 10 June at the Wenyiguan site and at 22 pm on 23 June at the Gaoqiao site, respectively. For the site with few ships (Fig. 9c), the simulations of both LMSE and LHSE showed false peaks, but the peak values using LMSE were much higher than those using LHSE, and the change trend of SO₂ concentrations by LHSE was more consistent with the measurements. In addition, we determined the vertical profiles of SO₂ at the Wenyiguan (Ningbo) and Gaoqiao (Shanghai) coastal sites (shown in Fig. 10). The concentrations of SO₂ distributed from the surface to ~1000 m showed a tendency similar to the trend of the surface SO₂ concentrations. These results confirm that ship emissions with a refined temporal resolution are needed to accurately reproduce modeling simulations.

4. Conclusions and discussions

In this study, the impacts of different temporal resolutions for ship emissions on coastal air quality simulations were investigated with continuous measurements along a ship cruise route over the East China Sea to constrain the simulations.

The total monthly ship emissions of PM_{2.5}, SO₂, and NO_x in June 2017 based on AIS data over the YRD were 1.3×10^3 t, 9.3×10^3 t, and 3.7×10^4 t, respectively. There were large differences in hourly variations, and clear diurnal variations were also detected, such as those in the average hourly emissions fluxes of 1082.41 ± 444.41 and 593.55 ± 404.95 g/h/km² at the Yangtze Estuary near Waigaoqiao Port and the Ningbo-Zhoushan channel, respectively. High ship emission fluxes were observed primarily in inland areas near water bodies, major shipping lanes along coastlines, and harbor areas.

The influences of ship emissions on SO₂ and NO₂ were limited mainly to regions near shipping lanes. Ships contributed significantly to the SO₂, NO₂, and PM_{2.5} concentrations in Shanghai Port and Ningbo Port, reaching 6.64 ppbv, 13.92 ppbv, and 6.96 µg/m³ (54.47%, 52.0%, and 10.61% of PM_{2.5} by LMSE), respectively, in Shanghai Port and 2.15 ppbv, 8.79 ppbv, and 0.28 µg/m³ (80.72%, 81.79%, and 1.51% of SO₂, NO₂, and PM_{2.5} by LMSE), respectively, in Ningbo Port. Comparisons of the air quality simulations with measurements indicate that the simulations with hourly ship emissions were much better than those with monthly ship emissions for SO₂, with an NMB of 8.35% by LHSE. Simulations during ship-related periods with hourly ship emissions were most consistent with the observations, with NMBs decreasing from -43.03%, 301.49%, and 223.02% by LMSE to -27.28%, 90.45%, and 167.52% for PM_{2.5}, SO₂, and NO₂, respectively, by LHSE. This finding highlights the importance of using ship emissions with a fine temporal resolution, especially for SO₂. In addition, the simulations using hourly ship emissions obviously performed better for all pollutants than those using monthly ship emissions in harbor areas with high ship activities, and decreased

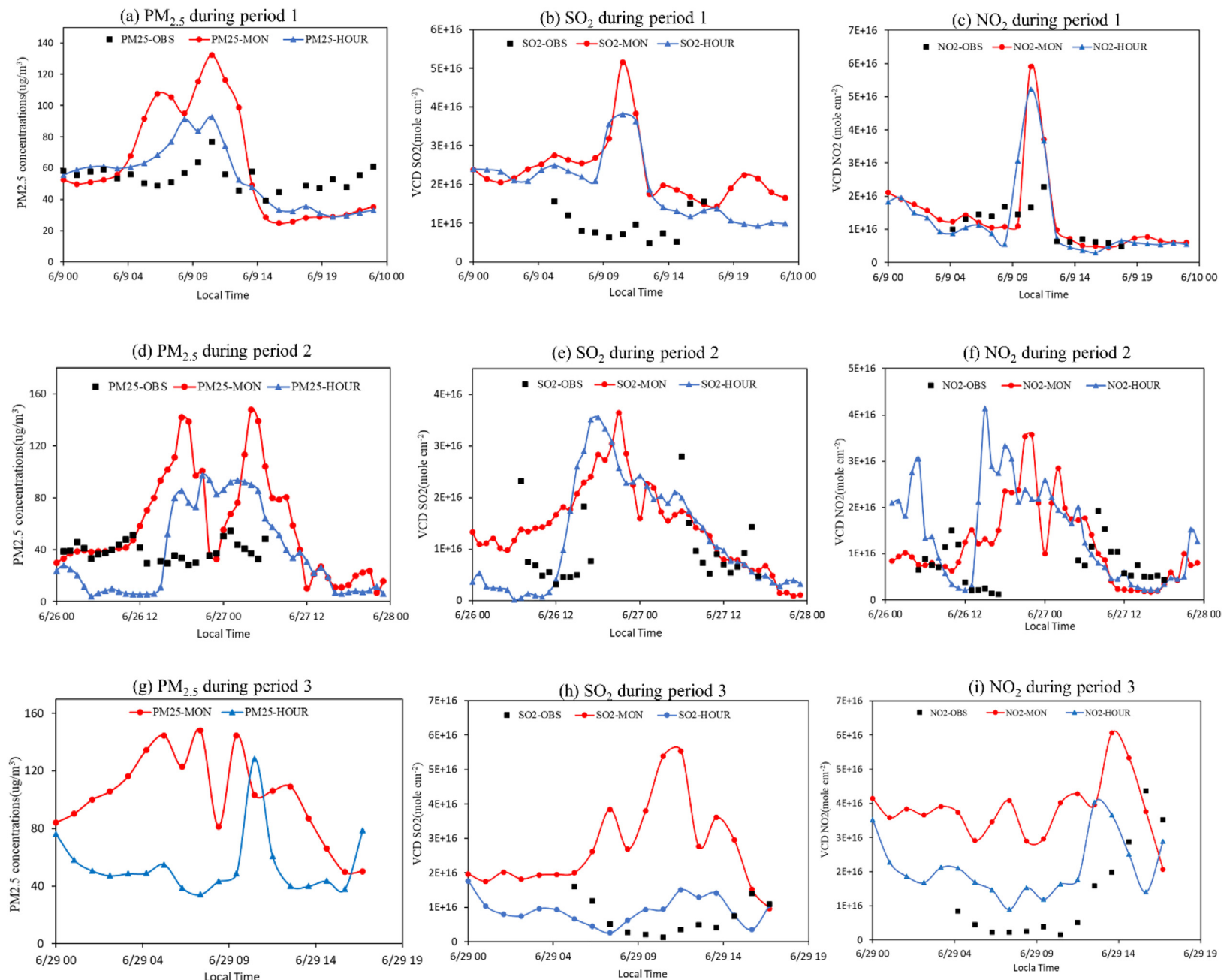


Fig. 7. Comparisons of surface concentrations of PM_{2.5}, column concentrations of SO₂ and NO₂ with LMSE and LHSE in the three periods shown in Fig. 1b. Black scatters represents observations; red scatters and lines represent simulations with monthly (June 2017) ship emission (LMSE); blue scatters and lines represent simulations with hourly ship emission (LHSE).

Table 2

NMBS of surface PM_{2.5}, and column SO₂ and NO₂ in domain 3 during the three periods.

Cases	Variables	No. samples	Obs. ave	Sim_Month.ave	Sim_Hour.ave	NMB_Month	NMB_Hour
Period 1	PM _{2.5}	24	53.78	62.74	54.27	16.67	0.93
	SO ₂	12	9.52E+15	2.63E+16	2.26E+16	175.81	137.73
	NO ₂	14	1.13E+16	1.46E+16	1.39E+16	28.68	22.50
Period 2	PM _{2.5}	28	38.97	72.08	46.48	84.96	19.27
	SO ₂	23	9.21E+15	1.35E+16	1.09E+16	49.29	21.16
	NO ₂	27	7.49E+15	8.20E+15	1.08E+16	9.52	43.89
Period 3	PM _{2.5}	-	-	-	-	-	-
	SO ₂	12	7.01E+15	3.14E+16	8.55E+15	348.33	22.01
	NO ₂	13	1.34E+16	3.81E+16	2.06E+16	185.13	54.29

Notes: the unit of Obs.ave. and Sim.ave. for PM_{2.5}: ug/m³, the unit of Obs.ave. and Sim.ave. for SO₂ and NO₂: molec cm⁻², the unit of NMB: %.

peak values, making the values closer to the measurements. Modeling simulations using monthly ship emissions will produce over- or underestimations if hourly fluctuations in the ship emission inventory are disregarded. Our research results showed the merit of hourly ship emission inventory, will promote the real-time ship emission inventory's application in coastal air quality management in near future.

There is a need to note that uncertainties in ship emissions, including the lack of AIS data, inland vessels without an AIS and the lack of estimated ship emission factors, meteorology, and photochemical processes, can all impact the simulations in the present study. In addition, we did not take the nonlinear chemistry of NOx and microphysics of aerosols in ship plumes into consideration in

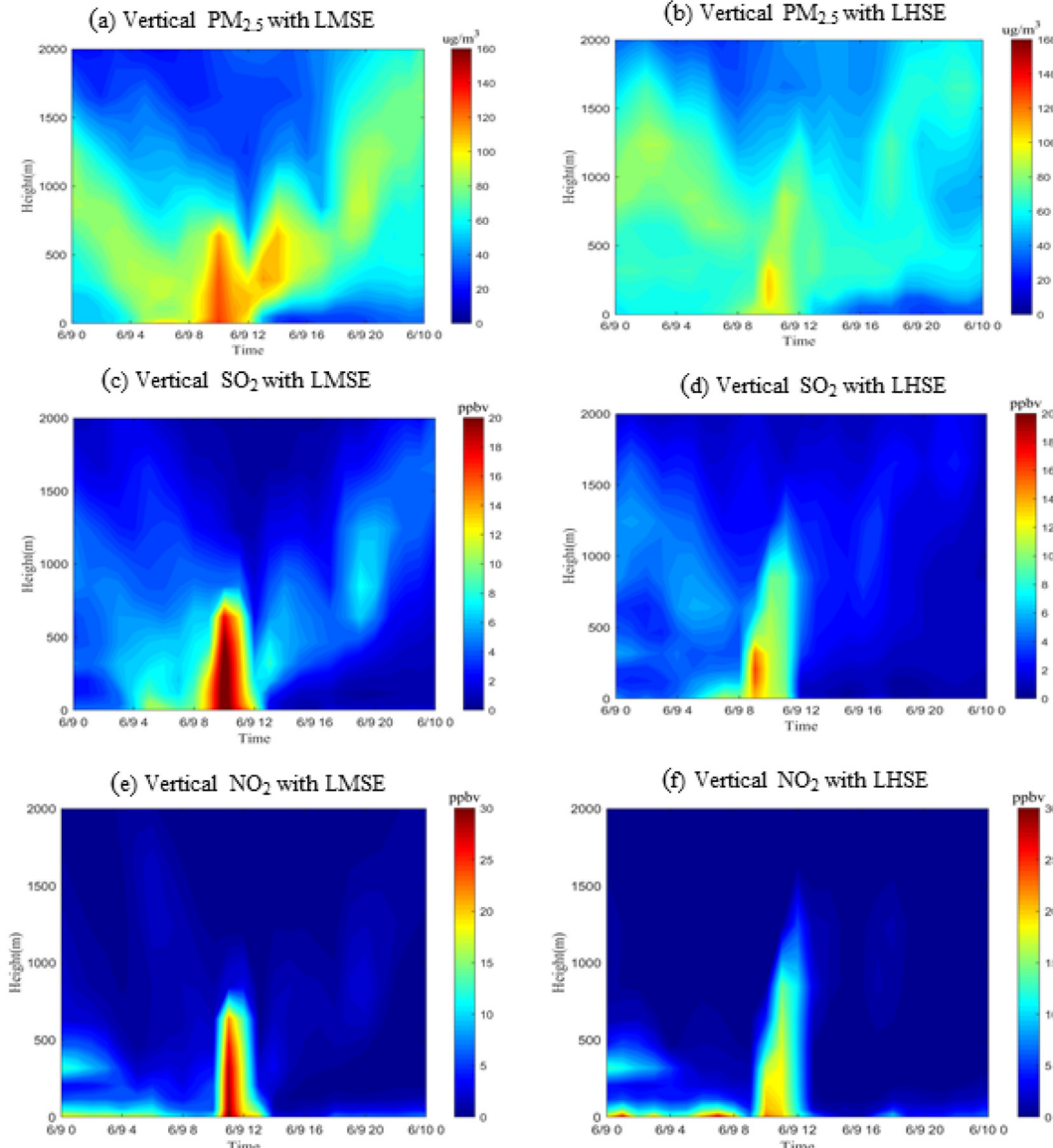


Fig. 8. Vertical profiles of PM_{2.5}, SO₂, and NO₂ (up to down) during period 1 on 9 June, when the ship was passing through Ningbo-Zhoushan channel. Left panels represent the results with monthly (June 2017) ship emission (LMSE), while right panels show the simulations with hourly ship emission (LHSE).

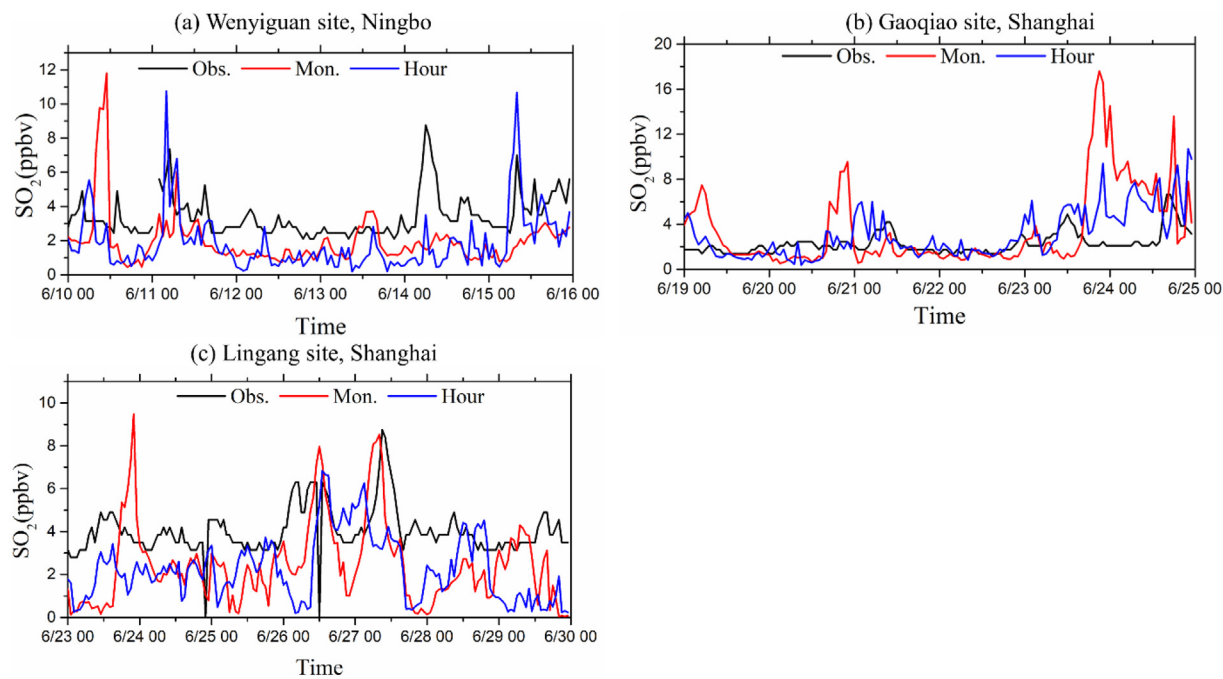


Fig. 9. Comparisons of modeled SO_2 concentrations by monthly (June 2017) ship emission (LMSE) and hourly ship emission (LHSE) with observations at (a) Wenyiguan, Ningbo; (b) Gaoqiao, Shanghai; and (c) Lingang, Shanghai, respectively.

the present modeling simulation since dilution process of ship plumes ignored, and this neglect may have resulted in the overestimation of NO_x , as one study reported that ignoring the nonlinear chemistry of NO_x in the initial dispersion stage of fresh ship exhaust could lead to heavily overestimated NO_x and O_3 concentrations (Davis et al., 2001). To advance the accuracy of 3-D modeling simulations, the sub-in-grid process of ship emissions needs to be considered in future work, which also calls for the real-time ship emission inventory.

CRediT authorship contribution statement

Jingbo Mao:Writing - original draft, Investigation, Methodology, Software, Validation, Formal analysis, Data curation, Visualization.**Yan Zhang:**Conceptualization, Investigation, Supervision, Methodology, Validation, Formal analysis, Writing - review & editing, Project administration, Funding acquisition.**Fangqun Yu:**Validation, Investigation, Writing - review & editing.**Jianmin Chen:**Resources, Data curation, Investigation, Writing - review & editing.**Jianfeng Sun:**Data curation,

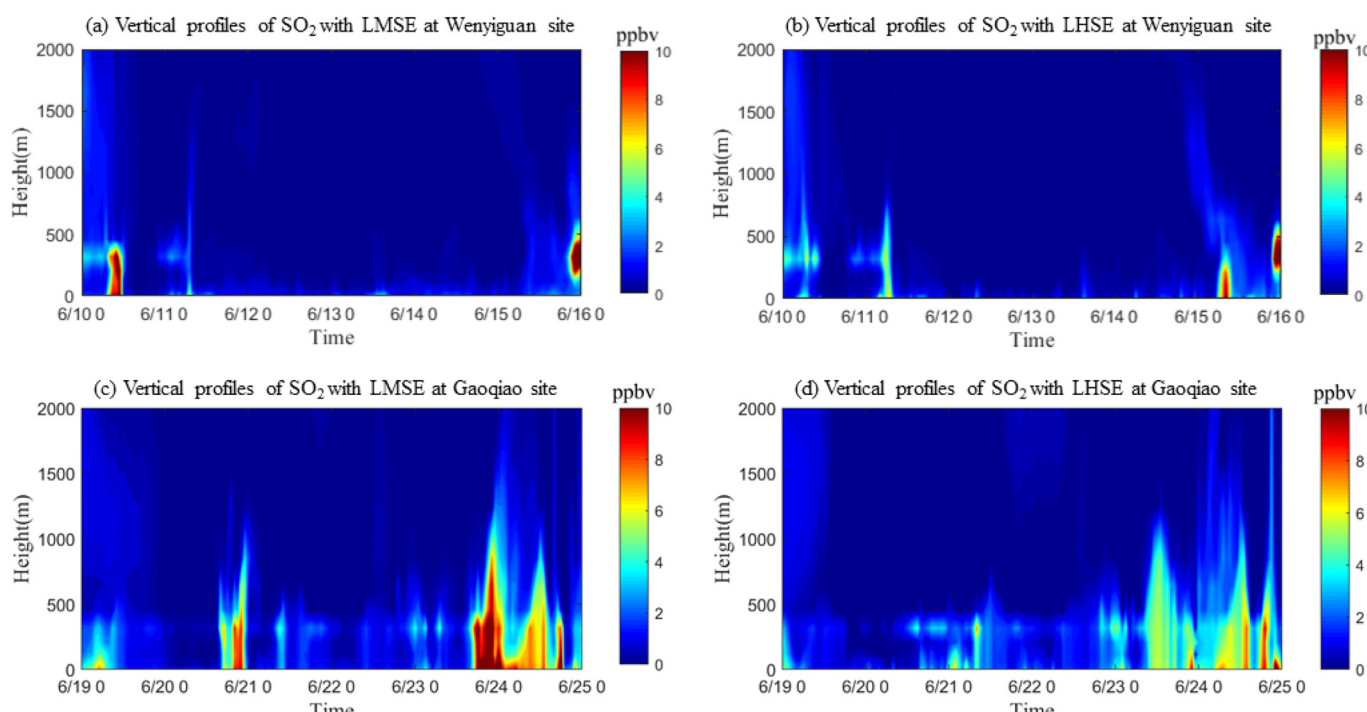


Fig. 10. Vertical profiles of SO_2 at Wenyiguan (a,b) and Gaoqiao sites (c, d). Left panels represent the results with monthly (June 2017) ship emission (LMSE), while right panels show the simulations with hourly ship emission (LHSE).

Investigation, Writing - review & editing. **Shanshan Wang**: Data curation, Writing - review & editing. **Zhong Zou**: Investigation, Data curation, Writing - review & editing. **Jun Zhou**: Investigation, Data curation, Writing - review & editing. **Qi Yu**: Validation, Investigation, Writing - review & editing. **Weichun Ma**: Investigation, Writing - review & editing. **Limin Chen**: Conceptualization, Investigation, Validation, Writing - review & editing.

Declaration of competing interest

The authors declare that they have no conflict of interest.

Acknowledgments

This work was supported by the National Natural Science Foundation of China (21677038), the National Key Research and Development Program of China (2016YFA060130X) and the Major Program of Shanghai Committee of Science and Technology, China (No.17DZ1202900 and No.19DZ1205009). Thanks are extended to the Maritime Safety Administration of Shanghai and the International Ship Center by providing the AIS data used in this study.

Appendix A. Supplementary data

Supplementary data to this article can be found online at <https://doi.org/10.1016/j.scitotenv.2020.138454>.

References

- Capaldo, K., Corbett, J.J., Kasibhatla, P., Fischbeck, P., Pandis, S.N., 1999. Effects of ship emissions on sulphur cycling and radiative climate forcing over the ocean. *Nature* 400, 743. <https://doi.org/10.1038/23438>.
- Chen, D., Wang, X., Li, Y., Lang, J., Zhou, Y., Guo, X., Zhao, Y., 2017a. High-spatiotemporal-resolution ship emission inventory of China based on AIS data in 2014. *Sci. Total Environ.* 609, 776–787. <https://doi.org/10.1016/j.scitotenv.2017.07.051>.
- Chen, D., Wang, X., Nelson, P., Li, Y., Zhao, N., Zhao, Y., Lang, J., Zhou, Y., Guo, X., 2017b. Ship emission inventory and its impact on the PM_{2.5} air pollution in Qingdao port, North China. *Atmos. Environ.* 166, 351–361. <https://doi.org/10.1016/j.atmosenv.2017.07.021>.
- Chen, D., et al., 2018. Contribution of ship emissions to the concentration of PM_{2.5}: A comprehensive study using AIS data and WRF/Chem model in Bohai Rim Region, China. *Sci. Total Environ.* 610, 1476–1486.
- Chen, D., Tian, X., Lang, J., Zhou, Y., Li, Y., Guo, X., Wang, W., Liu, B., 2019. The impact of ship emissions on PM_{2.5} and the deposition of nitrogen and sulfur in Yangtze River Delta, China. *Sci. Total Environ.* 649, 1609–1619. <https://doi.org/10.1016/j.scitotenv.2018.08.313>.
- Cooper, D., 2003. Exhaust emissions from ships at berth. *Atmos. Environ.* 37, 3817–3830. [https://doi.org/10.1016/S1352-2310\(03\)00446-1](https://doi.org/10.1016/S1352-2310(03)00446-1).
- Corbett, J.J., Fischbeck, P., 1997. Emissions from ships. *Science* 278 (278), 823–824.
- Corbett, J.J., Koehler, H.W., 2003. Updated emissions from ocean ship. *J. Geophys. Res.-Atmos.* 108, 4650. <https://doi.org/10.1029/2003JD003751>.
- Corbett, J.J., Fischbeck, P.S., Pandis, S.N., 1999. Global nitrogen and sulfur emissions inventories for oceangoing ships. *J. Geophys. Res.* 104 (D3), 3457–3470.
- Davis, D.D., Grodzinsky, G., Kasibhatla, P., Crawford, J., Chen, G., Liu, S., Bandy, A., Thornton, D., Guan, H., Sandholm, S., 2001. Impact of ship emissions on marine boundary layer NO_x and SO₂ distributions over the Pacific Basin. *Geophys. Res. Lett.* 28, 235–238.
- de Meij, A., Krof, M., Dentener, F., Vignati, E., Cuvelier, C., Thunis, P., 2006. The sensitivity of aerosol in Europe to two different emission inventories and temporal distribution of emissions. *Atmos. Chem. Phys.* 6, 4287–4309. <https://doi.org/10.5194/acp-6-4287-2006>.
- Ding, J., van der A, R.J., Mijling, B., Jalkanen, J.-P., Johansson, L., Levelt, P.F., 2018. Maritime NO_x emissions over Chinese seas derived from satellite observations. *Geophys. Res. Lett.* 45, 2031–2037. <https://doi.org/10.1002/2017GL076788>.
- ESRI: ArcGIS 10.2. Environmental Systems Research Institute Inc, Redlands.
- Eyring, V., Köhler, H.W., Aardenne, J.V., 2005. Emissions from international ship: 1. The last 50 years. *J. Geophys. Res. Atmos.* 110, 3928–3950.
- Eyring, V., Isaksen, I.S., Berntsen, T., Collins, W.J., Corbett, J.J., Endresen, O., Grainger, R.G., Moldanova, J., Schlager, H., Stevenson, D.S., 2010. Transport impacts on atmosphere and climate: ship. *Atmos. Environ.* 44, 4735–4771. <https://doi.org/10.1016/j.atmosenv.2009.04.059>.
- Fan, Q., Zhang, Y., Ma, W., Ma, H., Feng, J., Yu, Q., Yang, X., Ng, S.K., Fu, Q., Chen, L., 2016. Spatial and seasonal dynamics of ship emissions over the Yangtze River Delta and East China Sea and their potential environmental influence. *Environ. Sci. Technol.* 50, 1322–1329. <https://doi.org/10.1021/acs.est.5b03965>.
- Feng, J., Zhang, Y., Li, S., Mao, J., Patton, A.P., Zhou, Y., Ma, W., Liu, C., Kan, H., Huang, C., An, J., Li, L., Shen, Y., Fu, Q., Wang, X., Liu, J., Wang, S., Ding, D., Cheng, J., Ge, W., Zhu, H., Walker, K., 2019. The influence of spatiality on ship emissions, air quality and potential human exposure in the Yangtze River Delta/Shanghai, China. *Atmos. Chem. Phys.* 19, 6167–6183. <https://doi.org/10.5194/acp-19-6167-2019>.
- Gariazzo, C., et al., 2007. Application of a Lagrangian particle model to assess the impact of harbour, industrial and urban activities on air quality in the Taranto area, Italy. *Atmos. Environ.* 41 (30), 6432–6444.
- Gilliland, A.B., Dennis, R.L., Roselle, S.J., Pierce, T.E., 2003. Seasonal NH₃ emission estimates for the eastern United States based on ammonium wet concentrations and an inverse modeling method. *J. Geophys. Res.* 108 (D15), 4477. <https://doi.org/10.1029/2002JD003063>.
- Goldsworthy, Brett, Enshaei, Hossein, Jayasinghe, Shantha, 2019. Comparison of large-scale ship exhaust emissions across multiple resolutions: from annual to hourly data. *Atmos. Environ.* 214, 116829. <https://doi.org/10.1016/j.atmosenv.2019.116829>.
- Grell, G.A., Peckham, S.E., Schmitz, R., McKeen, S.A., Frost, G., Skamarock, W.C., Eder, B., 2005. Fully coupled “online” chemistry within the WRF model. *Atmos. Environ.* 39, 6957–6975.
- Guenther, A., Karl, T., Harley, P., Wiedinmyer, C., Palmer, P.I., Geron, C., 2006. Estimates of global terrestrial isoprene emissions using MEGAN (Model of Emissions of Gases and Aerosols from Nature). *Atmos. Chem. Phys.* 6, 3181–3210. <https://doi.org/10.5194/acp-6-3181-2006>.
- Heo, J., Adams, P.J., Gao, H.O., 2017. Public health costs accounting of inorganic PM_{2.5} pollution in metropolitan areas of the United States using a risk-based source-receptor model. *Environ. Int.* 106, 119–126.
- Johansson, L., Jalkanen, J.-P., Kukkonen, J., 2017. Global assessment of ship emissions in 2015 on a high spatial and temporal resolution. *Atmos. Environ.* 167, 403–415. <https://doi.org/10.1016/j.atmosenv.2017.08.042>.
- Karl, M., Jonson, J.E., Uppstu, A., Aulinger, A., Prank, M., Sofiev, M., Jalkanen, J.-P., Johansson, L., Quante, M., Matthias, V., 2019. Effects of ship emissions on air quality in the Baltic Sea region simulated with three different chemistry transport models. *Atmos. Chem. Phys.* 19, 7019–7053. <https://doi.org/10.5194/acp-19-7019-2019>.
- Lawrence, M.G., Crutzen, P.J., 1999. Influence of NO_x emissions from ships on tropospheric photochemistry and climate. *Nature* 402 (6758), 167–170.
- Li, M., Zhang, D., Li, C.-T., Mulvaney, K.M., Selin, N.E., Karplus, V.J., 2018. Air quality co-benefits of carbon pricing in China. *Nat. Clim. Chang.* 8, 398. <https://doi.org/10.1038/s41558-018-0139-4>.
- Liu, H., Fu, M., Jin, X., Shang, Y., Shindell, D., Faluvegi, G., Shindell, C., He, K., 2016a. Health and climate impacts of oceangoing vessels in East Asia. *Nat. Clim. Chang.* 6, 1037–1041. <https://doi.org/10.1038/nclimate3083>.
- Liu, Z., Lu, X., Feng, J., Fan, Q., Zhang, Y., Yang, X., 2016b. Influence of ship emissions on urban air quality: a comprehensive study using highly time-resolved online measurements and numerical simulation in Shanghai. *Environ. Sci. Technol.* 51, 202–211. <https://doi.org/10.1021/acs.est.6b03834>.
- Lv, Z., Liu, H., Ying, Q., Fu, M., Meng, Z., Wang, Y., Wei, W., Gong, H., He, K., 2018. Impacts of ship emissions on PM_{2.5} pollution in China. *Atmos. Chem. Phys.* 18, 15811–15824. <https://doi.org/10.5194/acp-18-15811-2018>.
- Mao, J., Yu, F., Zhang, Y., An, J., Wang, L., Zheng, J., Yao, L., Luo, G., Ma, W., Yu, Q., Huang, C., Li, L., Chen, L., 2018. High-resolution modeling of gaseous methylamines over a polluted region in China: source-dependent emissions and implications of spatial variations. *Atmos. Chem. Phys.* 18, 7933–7950. <https://doi.org/10.5194/acp-18-7933-2018>.
- Marelle, L., Thomas, J.L., Raut, J.-C., Law, K.S., Jalkanen, J.-P., Johansson, L., Roiger, A., Schlager, H., Kim, J., Reiter, A., Weinzierl, B., 2016. Air quality and radiative impacts of Arctic ship emissions in the summertime in northern Norway: from the local to the regional scale. *Atmos. Chem. Phys.* 16, 2359–2379. <https://doi.org/10.5194/acp-16-2359-2016>.
- Poplawski, K., et al., 2011. Impact of cruise ship emissions in Victoria, BC, Canada. *Atmos. Environ.* 45 (4), 824–833.
- Sofiev, M., Winebrake, J.J., Johansson, L., Carr, E.W., Prank, M., Soares, J., Vira, J., Kouznetsov, R., Jalkanen, J.-P., Corbett, J.J., 2018. Cleaner fuels for ships provide public health benefits with climate tradeoffs. *Nat. Commun.* 9, 406. <https://doi.org/10.1038/s41467-017-02774-9>.
- Stohl, A., Aamaas, B., Amann, M., Baker, L.H., Bellouin, N., Berntsen, T.K., Boucher, O., Cherian, R., Collins, W., Daskalakis, N., Dusinska, M., Eckhardt, S., Fuglestvedt, J., S. Harju, M., Heyes, C., Hodnebrog, Ø., Hao, J., Im, U., Kanakidou, M., Klimont, Z., Kupiainen, K., Law, K.S., Lund, M.T., Maas, R., MacIntosh, C.R., Myhre, G., Myriokefalitakis, S., Olivie, D., Quaas, J., Quennhenen, B., Raut, J.C., Rumbold, S.T., Samset, B.H., Schulz, M., Seland, Ø., Shine, K.P., Skeie, R.B., Wang, S., Yttri, K.E., Zhu, T., 2015. Evaluating the climate and air quality impacts of short-lived pollutants. *Atmos. Chem. Phys.* 15, 10529–10566. <https://doi.org/10.5194/acp-15-10529-2015>.
- Tan, J., Zhang, Y., Ma, W., Yu, Q., Wang, J., Chen, L., 2015. Impact of spatial resolution on air quality simulation: A case study in a highly industrialized area in Shanghai, China. *Atmos. Pollut. Res.* 6, 322–333.
- Tan, W., Liu, C., Wang, S., Xing, C., Su, W., Zhang, C., Xia, C., Liu, H., Cai, Z., Liu, J., 2018. Tropospheric NO₂, SO₂, and HCHO over the East China Sea, using ship-based MAX-DOAS observations and comparison with OMI and OMPS satellite data. *Atmos. Chem. Phys.* 18, 15387–15402. <https://doi.org/10.5194/acp-18-15387-2018>.
- Thornton, J.A., Virts, K.S., Holzworth, R.H., Mitchell, T.P., 2017. Lightning enhancement over major oceanic ship lanes. *Geophys. Res. Lett.* 44, 9102–9111. <https://doi.org/10.1002/2017GL074982>.
- UNCTAD: Review of Maritime Transport 2017, available at: https://unctad.org/en/PublicationsLibrary/rmt2017_en.pdf (last access: 4 June 2019), United Nations Publication, USA, 2017.

- Wang, X., Shen, Y., Lin, Y., Pan, J., Zhang, Y., Louie, P.K.K., Li, M., Fu, Q., 2019. Atmospheric pollution from ships and its impact on local air quality at a port site in Shanghai. *Atmos. Chem. Phys.* 19, 6315–6330. <https://doi.org/10.5194/acp-19-6315-2019>.
- Zhang, X., Zhang, Y., Liu, Y., et al., 2019. Changes in the SO₂ Level and PM_{2.5} Components in Shanghai Driven by Implementing the Ship Emission Control Policy. *Environ. Sci. Technol* 53 (19), 11580–11587.
- Zhao, M., Zhang, Y., Ma, W., Fu, Q., Yang, X., Li, C., Zhou, B., Yu, Q., Chen, L., 2013. Characteristics and ship traffic source identification of air pollutants in China's largest port. *Atmos. Environ.* 64, 277–286. <https://doi.org/10.1016/j.atmosenv.2012.10.007>.
- Zhao, B., Zheng, H., Wang, S., Smith, K.R., Lu, X., Aunan, K., Gu, Y., Wang, Y., Ding, D., Xing, J., Fu, X., Yang, X., Liou, K.N., Hao, J., 2018. Change in household fuels dominates the decrease in PM_{2.5} exposure and premature mortality in China in 2005–2015. *P. Natl. Acad. Sci. USA* 115, 12401–12406. <https://doi.org/10.1073/pnas.1812955115>.